


Exchange-Correlation Effects and the Quasiparticle Properties in a Two-Dimensional Dipolar Fermi Liquid

Iran Seydi¹ · Saeed H. Abedinpour^{1,2} · Reza Asgari^{2,3} · B. Tanatar⁴ 

Received: 7 November 2019 / Accepted: 21 November 2019 / Published online: 17 December 2019
© Springer Science+Business Media, LLC, part of Springer Nature 2019

Abstract

We investigate the effects of exchange and correlation on the quasiparticle properties such as the self-energy, the many-body effective mass and the renormalization constant in a two-dimensional system of ultracold dipolar fermions with dipole moments aligned in the perpendicular direction to the plane. We use the G_0W approximation along with the generalized random phase approximation, where the many-body effects have been incorporated in the effective interaction W through the Hubbard local-field factor. The many-body effective mass and the renormalization constant are reduced with the increase of coupling strength. We also study the effect of dipole-dipole interaction on the single-particle spectral function of the two dimensional dipolar Fermi liquid. We observe composite hole-zero sound excitation which is a bound state of quasiparticles with the collective mode (i.e. zero-sound) at intermediate and high coupling constants. These composite excitations are undamped at small wave vectors. Due to repulsion between quasiparticle and composite excitation resonances, we find a gap-like feature between quasiparticle and composite excitation dispersions at long wavelengths.

Keywords Dipolar Fermi liquid · G_0W · Effective mass · Renormalization constant · Spectral function · Composite quasiparticles

1 Introduction

Ultracold atomic gases are classified as a member of relatively strongly correlated systems due to their long-range and anisotropic interactions [1, 2]. They have many interesting applications in chemical reactions, quantum information and novel quantum phase transitions [3–6]. Instabilities occur in dipolar quantum gases when interactions are sufficiently strong and attractive [7–9]. The long-range interaction leads to the emergence of a variety of quantum phases [2, 10, 11]. The many-body

effects in these quantum gases have been investigated by various groups. In this respect, Fermi liquid properties in the two-dimensional (2D) polar molecules have been studied by many-body perturbation theory [12], quantum Monte Carlo [13] and G_0W [14, 15] methods. Also, the ground-state properties and density wave instability [16–18] in a two-dimensional (2D) dipolar Fermi gas have been studied in the framework of Hartree-Fock [19], improved Sigwi-Tosi-Land-Sjölander [20] and Fermi-hypernetted-chain (FHNC) [21] approximations.

Low-energy dynamical properties of a Fermi system is phenomenologically described by means of the Landau's Fermi-liquid theory [22, 23]. Polar particles in a dipolar Fermi gas exhibit dipole-dipole interactions, in which independent particles are replaced by quasiparticles (QP) interacting via dynamically screened dipole-dipole interaction. Screened interactions lead to the modification of band energy. This modification is extracted from the self-energy function. In this paper, we study the effect of dipole-dipole interaction on the quasiparticle properties of a 2D dipolar Fermi liquid within the G_0W approximation to the self-energy while using the Hubbard local-field factor (LFF) [23] to account for the exchange effects in the effective interaction.

✉ B. Tanatar
tanatar@fen.bilkent.edu.tr

¹ Department of Physics, Institute for Advanced Studies in Basic Sciences (IASBS), Zanjan, 45137-66731, Iran

² School of Nano Science, Institute for Research in Fundamental Sciences (IPM), Tehran, 19395-5531, Iran

³ School of Physics, Institute for Research in Fundamental Sciences (IPM), Tehran, 19395-5531, Iran

⁴ Department of Physics, Bilkent University, Bilkent, 06800, Ankara, Turkey

Band structure and single-particle excitations in a correlated quantum fluid are obtained from the single-particle spectral function. Dynamics of quantum systems have been studied extensively over the past decades. Dynamical properties have been investigated in the electron gas [24, 25] and graphene [26–31], and the observation of plasmaron excitations has been reported in graphene [32]. Composite hole-acoustic plasmon satellite bands have been predicted for a graphene sheet on a metallic gate [33]. Godfrin and coworkers studied the dynamical properties of a monolayer of liquid ^3He by means of inelastic neutron scattering measurements and they reported the observation of a roton-like excitation [34]. The dynamical properties of 2D dipolar Fermi gases have been studied in our recent work and we have reported the formation of composite quasiparticles [15] using FHNC results for the static structure factor to extract the many-body effective interaction.

In this work, we aim to test the effects of using a much simple form of the effective interaction, i.e. using the Hubbard approximation for the LFF, on the QP properties and the single-particle spectral function in a 2D dipolar Fermi liquid. The main advantage of this method is that it does not rely on any input from other more sophisticated calculations, such as quantum Monte-Carlo (QMC) or FHNC for the ground state properties. Therefore, it is easily applicable for other systems with other forms of interactions where such input is not available.

The rest of the paper is organized as follows. In Section 2, we introduce our model and give the details of the method we use to calculate the QP properties and single-particle spectral function. In Section 3, we illustrate our numerical results for QP properties and spectral function. Finally, in Section 4, we give a summary and conclude our results.

2 Theory

We consider a 2D single-layer gas of spin-polarized dipolar fermions with their dipole moments aligned in the perpendicular direction to the 2D plane. The isotropic bare dipole-dipole interaction between particles reads

$$v_{\text{dd}}(r) = \frac{C_{\text{dd}}}{4\pi} \frac{1}{r^3}. \quad (1)$$

Here, C_{dd} is the dipole-dipole coupling constant, which is d^2/ϵ_0 for molecules with permanent electric dipole d and $\mu_0 M^2$ for atoms with permanent magnetic dipole M , where ϵ_0 and μ_0 are the permittivity and permeability of vacuum, respectively. At zero temperature, all the properties of this dipolar system will depend on a single dimensionless coupling constant $\lambda = k_F r_0$, where $r_0 = m C_{\text{dd}} / (4\pi \hbar^2)$ is a characteristic length of dipolar interaction and $k_F = \sqrt{4\pi n}$

is the Fermi wave vector with n being the 2D density. Note that here m is the bare (i.e., non-interacting) mass of dipoles, and the system is spin polarized. We assume low-lying excitations and resort to the G_0W approximation for the self-energy [23]

$$\Sigma(k, E) = i \int \frac{d^2 \mathbf{q} d(\hbar\omega)}{(2\pi)^3} G^0(\mathbf{k} - \mathbf{q}, E - \hbar\omega) W(q, \omega). \quad (2)$$

In order to account for the exchange and correlation effects, $W(q, \omega)$ is approximated by the Kukkonen-Overhauser (KO) effective interaction [23]

$$W(q, \omega) = v(q) + w^2(q, \omega) \chi(q, \omega), \quad (3)$$

where $v(q)$ is the Fourier transform of bare interaction $v_{\text{dd}}(r)$, and $\chi(q, \omega)$ is the density-density linear response function. Within a generalized random-phase approximation (RPA), the density-density response function could be expressed as [23]

$$\chi(q, \omega) = \frac{\chi_0(q, \omega)}{1 - w(q, \omega) \chi_0(q, \omega)}, \quad (4)$$

where $\chi_0(q, \omega)$ is the density-density response function of an ideal (i.e., non-interacting) 2D Fermi gas. The statically screened interaction $w(q)$ is defined through (4); however, in any practical application, it should be approximated. In the RPA, one normally replaces it with the bare interaction but in the case of dipolar interaction, this leads to an unphysical cutoff dependence of the interaction [15]. An accurate knowledge of the static structure factor of the interacting system through QMC or FHNC combined with the fluctuation-dissipation theorem leads to more accurate static approximations for the screened interaction [14, 15]. In the present work, we adopt an analytic approximation for the many-body LFF, namely the Hubbard approximation [23], which partially takes into account the effects of exchange hole

$$w_{\text{H}}(q) = v(q) - v \left(\sqrt{k_F^2 + q^2} \right). \quad (5)$$

The simplest approximation for obtaining the self-energy is the Hartree-Fock (HF) approximation in which only the exchange effect is included by keeping the first term on the right-hand-side of (3)

$$\Sigma^{\text{HF}}(k) = \int \frac{d^2 \mathbf{q}}{(2\pi)^2} [v(0) - v(\mathbf{k} - \mathbf{q})] n_{\text{FD}}[\epsilon(q)]. \quad (6)$$

Here, $n_{\text{FD}}(\epsilon)$ is the Fermi-Dirac distribution function and $\epsilon(k) = \hbar^2 k^2 / (2m)$ is the non-interacting dispersion of particles. Note that $v(0)$ which has been included in (6) accounts for the Hartree contribution to the self-energy. This term is absent in the jellium model of the electron gas [23] due to the charge neutrality, and is a trivial constant shift in the energy in other homogeneous systems. Here, while it has a constant k -independent value, its inclusion

is essential for canceling out a similar cutoff-dependent constant contribution from the exchange term.

The full self-energy in the framework of G_0W reads [15, 23]

$$\Sigma(k, E) = \Sigma^{\text{HF}}(k) + \Sigma^{(\rho)}(k, E), \quad (7)$$

which is split into two terms: the static mean-field, i.e. “Hartree-Fock” term $\Sigma^{\text{HF}}(k)$, and the dynamic term $\Sigma^{(\rho)}(k, E)$, which originates from density fluctuations. With the stated approximations, the excitation spectrum for quasiparticles is written as

$$\varepsilon_{\text{QP}}(k) = \xi(k) + \Re \tilde{\Sigma}(k, E)|_{E=\varepsilon_{\text{QP}}(k)}. \quad (8)$$

Here, $\xi(k) = \varepsilon(k) - \mu_0$ and $\Re \tilde{\Sigma}(k, E) = \Re \Sigma(k, E) - \Re \Sigma(k_F, 0)$, where μ_0 is the chemical potential of the non-interacting system. In the numerical calculations, we will use the “on-shell approximation” (OSA), replacing $\varepsilon_{\text{QP}}(k) \rightarrow \xi(k)$ in the self-energy [23, 35, 36]:

$$\varepsilon_{\text{QP}}^{\text{OSA}}(k) \simeq \xi(k) + \Re \tilde{\Sigma}(k, E)|_{E=\xi(k)}. \quad (9)$$

In the presence of interactions, discontinuity of the momentum distribution at the Fermi level, that is measured by the renormalization constant, is less than unity [23]

$$Z = \frac{1}{1 - \partial_E \Re \Sigma(k, E)|_{k=k_F, E=0}}. \quad (10)$$

The many-body effective mass at the Fermi level is obtained from the slope of interacting excitation spectrum [23]

$$\frac{1}{m^*} = \frac{1}{\hbar^2 k_F} \left. \frac{d\varepsilon_{\text{QP}}(k)}{dk} \right|_{k \rightarrow k_F}. \quad (11)$$

As the quasiparticle energy could be calculated either by solving the self-consistent Dyson (8) or by using the OSA, there are two corresponding expressions for the many-body effective mass: The effective mass m_D^* is obtained by self-consistently solving the Dyson equation [23, 35]

$$\frac{m}{m_D^*} = Z \left[1 + \frac{m}{\hbar^2 k_F} \partial_k \Re \Sigma(k, E)|_{k=k_F, E=0} \right], \quad (12)$$

while the many-body effective mass within the on-shell approximation could be written as [23, 35]

$$\frac{m}{m_{\text{OSA}}^*} = 1 + \frac{m}{\hbar^2 k_F} \partial_k \Re \Sigma(k, E)|_{k=k_F, E=0} + \partial_E \Re \Sigma(k, E)|_{k=k_F, E=0}. \quad (13)$$

The spectral function $A(\mathbf{k}, E)$, which plays a central role in the investigation of QP properties, is a useful physical quantity which is capable of providing information on band dispersion and Fermi surface. $A(\mathbf{k}, E)$ is the probability of finding a particle with momentum k and energy E . For a non-interacting system, the spectral function has a Dirac δ -function form. Interactions modify the single particle Green function $G^{-1}(k, E) = G_0^{-1}(k, E) - \Sigma(k, E)$, and the spectral function broadens to read $A(k, E) =$

$-\Im m G^{\text{ret}}(k, E)/\pi$. The renormalized spectral function is related to the self-energy and the non-interacting energy $\xi(k)$ through the equation [23, 37]

$$A(k, E) = \frac{-\Im m \Sigma(k, E)/\pi}{[E - \xi(k) - \Re \tilde{\Sigma}(k, E)]^2 + [\Im m \Sigma(k, E)]^2}. \quad (14)$$

The spectral function above has a Lorentzian shape where $\Re \tilde{\Sigma}(k, E)$ specifying the location of the peak of the distribution and the imaginary part of the self energy is the line-width. $A(k, E)$ is a positive-definite quantity and satisfies the sum rule $\int_{-\infty}^{\infty} A(k, E) dE = 1$. A fraction Z of the total spectral weight is absorbed by the QP peak and remaining $1 - Z$ is distributed over the background [23].

3 Numerical Results

We now turn to the presentation of our numerical results for the self-energy, renormalization constant and many-body effective mass. In Section 3.1, we present the results of the calculation of quasiparticle excitation energy and lifetime. In Section 3.2, we present the numerical results of the renormalization constant and many-body effective mass for two dimensional dipolar Fermi liquid and finally, in Section 3.3, we show the numerical results of the single-particle spectral function.

3.1 The Quasiparticle Self-Energy and Lifetime

The interaction between the particles in Fermi liquids, which leads to the quasiparticles have two important effects. First, the dynamical properties of quasiparticles such as energy dispersion relation and their mass are renormalized. Renormalized QP energy is determined by the real part of the self-energy. Second, the quasiparticles decay due to inelastic scatterings from other quasiparticles which leads to a finite lifetime. This QP lifetime is defined by the imaginary part of the self-energy. Figure 1 (top panel) shows the QP energy as a function of k obtained by on-shell approximation at different values of the coupling strength λ . For small coupling strengths, the system behaves very much like a non-interacting system because of the large cancellation between the static and dynamical contributions to the self-energy. In the intermediate and large coupling regimes, for $k < k_F$, the QP self-energy is slightly changed but for $k > k_F$ and at the k_c where the collective mode (i.e. zero-sound) emission occurs, the self-energy is abruptly decreased as the QP is allowed to emit collective modes. It then loses its energy and comes back near the Fermi surface. A strong dip in the real part of the self-energy is the zero-sound dip and it depends on the coupling strength

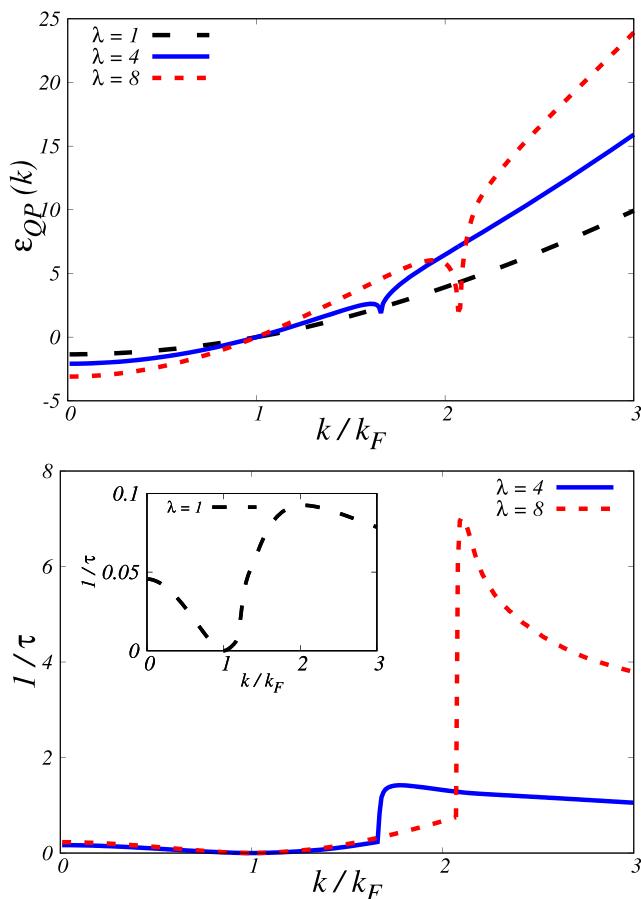


Fig. 1 Top: Quasiparticle energy (in units of ε_F) as a function of k at various coupling strengths. Bottom: The inverse of the quasiparticle lifetime (in units of $\hbar k_F^2/m$) as a function of k at different values of λ

λ . The position of zero-sound dip moves to larger k with increasing coupling strength. This zero-sound dip, which is similar to maxon-like dip reported in 2D ^3He [38, 39], and plasmon dip in 2D electron gas [35, 36] originates from the decay of particle-hole pair into a plasmon with conserved momentum and energy.

Two mechanisms exist for the scattering of a quasiparticle: excitation of particle-hole pairs, which is dominated at long wavelengths, and the excitation of zero-sound that turns on at a threshold wave vector k_c , where the collective mode dispersion enters the particle-hole continuum [24, 27]. In the bottom panel of Fig. 1, we present the inverse of the quasiparticle lifetime $\tau^{-1} = 2|\Im m \Sigma(k, \xi k)|/\hbar$ as a function of k for various values of λ evaluated in the OSA. The inverse of the quasiparticle lifetime vanishes at $k = k_F$, indicating that quasiparticles are well defined at the Fermi level, and the quasiparticle decay rate vanishes as $|k - k_F|^2$ for $k \rightarrow k_F$ that is one of the main features of the Fermi liquid theory [23]. A finite jump in the inverse lifetime takes place at the wave vector of zero-sound dip because at this wave vector the scattering rate is drastically increased. This jump

has also been reported for 2D electron gas [35] and there it arises from the non-zero oscillator strength of the plasmon pole at the wave number of plasmon dip. There is no zero-sound jump for small couplings (see, the inset in Fig. 1) but by increasing the coupling constant, the jump appears at k_c and by further increasing the coupling constant, the magnitude of the scattering rate and the wave vector at which the jump occurs change.

3.2 Renormalization Constant and Many-Body Effective Mass

The renormalization constant is the probability of removing or adding a particle at the Fermi energy without exciting the medium. Therefore, it is sensitive to the interaction strength. In Fig. 2 (top panel), we compare our numerical result for the renormalization constant with QMC results [13]. In the

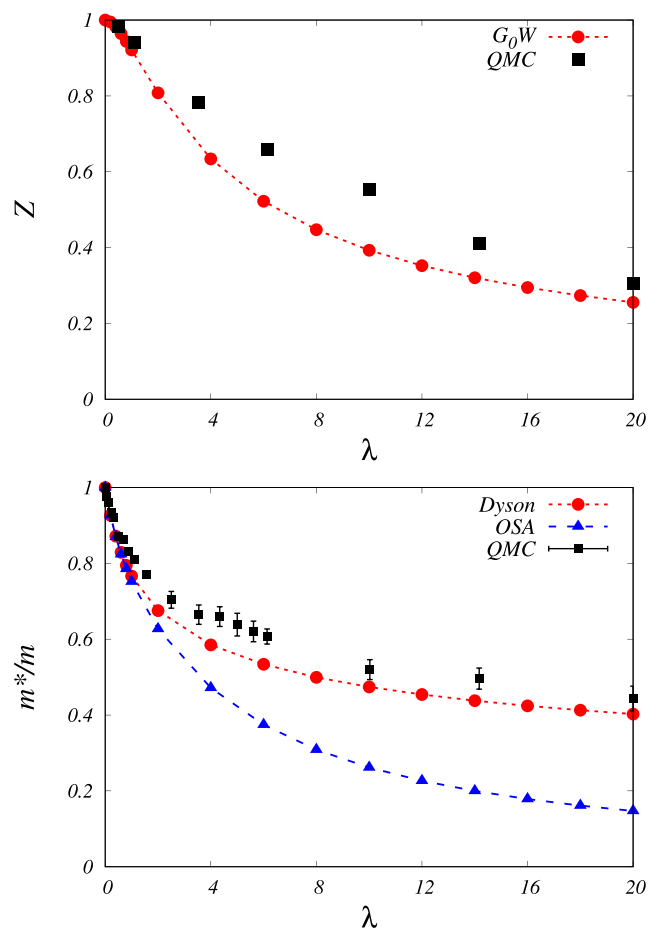


Fig. 2 Top: The renormalization constant of a 2D dipolar Fermi liquid as a function of the dimensionless coupling constant λ , calculated within the G_0W approximation and is compared with the QMC results of Ref. [13]. Bottom: The relative effective mass of a 2D dipolar Fermi liquid as a function of the dimensionless coupling constant λ , calculated within the on-shell and Dyson approximations for the G_0W formalism compared with the QMC results of Ref. [13]

weak coupling regime, the self-energy is dominated by the exchange effects. Because the Hartree-Fock self-energy is independent of energy, we expect in this regime Z to be close to its non-interacting value, i.e. $Z = 1$. As coupling constant increases, the effects of correlations become important and this leads to the reduction of renormalization constant. A large suppression of renormalization constant occurs at strong coupling, but Z never reaches zero. It could be taken as an indication of the Fermi liquid picture being maintained for this system as the Landau Fermi liquid theory implies $0 < Z \leq 1$.

A consequence of the electron-electron interaction is an effective mass renormalization from the backflow of the fluid around a moving particle. In the bottom panel of Fig. 2, we present our numerical results for the relative effective mass m^*/m and compare them with the QMC results [13]. Our calculations show the reduction of the effective mass in the entire range of coupling constants investigated. The Hartree-Fock contribution to the self-energy has a positive slope at k_F and hence decreases the effective mass, whereas the dynamic contribution to self-energy has a negative slope and tends to enhance the effective mass [14]. In the whole range of coupling strengths, the Hartree-Fock term dominates over the dynamical term hence the effective mass decreases. Evidently, the effective mass within the Dyson scheme is in very good agreement with the QMC results over the whole range of coupling strengths.

3.3 The Spectral Function

In this subsection, we present our numerical results for the many-body quasiparticle spectral function obtained from Eq. (14). When the first term in the denominator of Eq. (14) becomes zero, a resonance emerges in the spectral function that represents quasiparticles with a finite energy and lifetime. Figure 3 shows the spectral function versus energy for a 2D dipolar Fermi liquid at two different coupling constants and for several values of momenta. The spectral functions are slightly broadened (up to 0.005) to make the undamped delta-function like peaks visible.

For $\lambda = 1$, the spectral function has a single peak identified as the quasiparticle peak. This peak is broadened in comparison with a non-interacting system which has a delta-function peak. At $\lambda = 8$ and for small values of the wave vector, the spectral function features at least two pronounced peaks. If we account these peaks according to increasing distance from $E = 0$, the first peak is associated to the quasiparticle solution (i.e., a bare particle screened by a cloud of particle-hole excitations and collective modes) which is shifted from its non-interacting value and these peaks have finite widths corresponding to the non-zero damping rate that in turn results from the non-zero imaginary part of the many-body self-energy. The

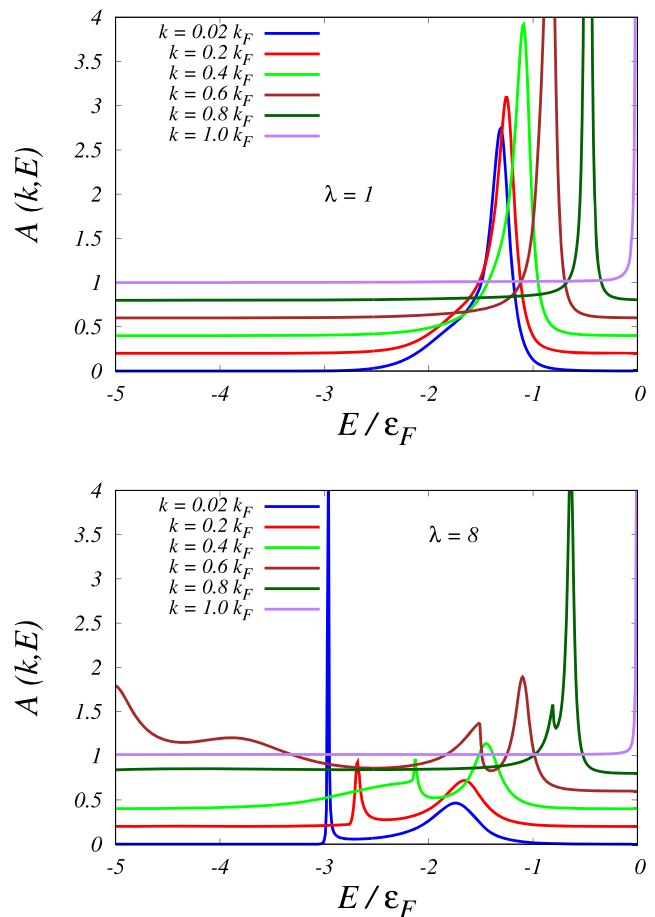


Fig. 3 The spectral function $A(k, E)$ as a function of the energy E at $\lambda = 1$ (top) and $\lambda = 8$ (bottom) and for six different values of the wave vector, $k = 0.02, 0.2, 0.4, 0.6, 0.8$ and $1.0 k_F$. Note that each curve of the spectral function has been shifted upwards by 0.2, with respect to the previous curve, for a better visibility

second peak results from the coupling of quasiparticles and collective modes. At long wavelengths, this composite quasiparticle becomes undamped and it gives rise to a δ -function peak in the spectral function. At larger values of wave vectors, when the dispersion of collective mode enters the particle-hole continuum and becomes vulnerable to the Landau damping, the composite quasiparticle peak eventually merges with the single particle peak and disappears.

4 Summary and Conclusions

We have calculated the quasiparticle properties such as the quasiparticle self-energy, quasiparticle lifetime, many-body effective mass and the renormalization constant of a spin-polarized 2D dipolar Fermi liquid. We have used G_0W approximation with a screened effective interaction

within the Hubbard approximation for the many-body local-field factor. Our effective mass results show reduction in the entire range of coupling strengths we have studied. A strong suppression of the renormalization constant occurs at strong couplings, but Z never reaches zero. It could be taken as an indication of the Fermi liquid picture being maintained in this system as the Landau Fermi liquid theory implies $0 < Z \leq 1$. We have also calculated the spectral function and we have observed composite quasiparticles consisting of a hole and zero-sound in the intermediate and high coupling regimes. Our theoretical results convincingly affirm the normal Fermi liquid nature of the 2D dipolar Fermi gas.

Funding Information BT acknowledges support from TUBA. SHA thanks TUBA for a travel grant during which this work is completed.

References

- Fregoso, B.M., Sun, K., Fradkin, E., Lev, B.L.: *J. Phys.* **11**, 103003 (2009)
- Baranov, M.A.: *Phys. Rep.* **464**, 71 (2008)
- Ni, K.-K., Ospelkaus, S., Wang, D., Quémener, G., Neyenhuis, B., de Miranda, M.H.G., Bohn, J.L., Ye, J., Jin, D.S.: *Nature* **464**, 1324 (2010)
- Ni, K.-K., Ospelkaus, S., Nesbitt, D.J., Ye, J., Jin, D.S.: *Phys. Chem. Chem. Phys.* **11**, 9626 (2009)
- de Miranda, M.H.G., Chotia, A., Neyenhuis, B., Wang, D., Quémener, G., Ospelkaus, S., Bohn, J.L., Ye, J., Jin, D.S.: *Nat. Phys.* **7**, 502 (2011)
- Carr, L.D., Demille, D., Krems, R.V., Ye, J.: *J. Phys.* **11**, 055049 (2009)
- Bruun, G.M., Taylor, E.: *Phys. Rev. Lett.* **101**, 245301 (2008)
- Astrakharchik, G.E., Boronat, J., Kurbakov, I.L., Lozovik, YuE.: *Phys. Rev. Lett.* **98**, 060405 (2007)
- Büchler, H.P., Demler, E., Micheli, M., Prokof'ev, N., Pupillo, G., Zoller, P.: *Phys. Rev. Lett.* **98**, 060404 (2007)
- Baranov, M.A., Dalmonte, M., Pupillio, G., Zoller, P.: *Chem. Rev.* **112**, 5012 (2012)
- Li, Y., Wu, C.: *J. Phys.: Condens. Matter* **26**, 493202 (2014)
- Lu, Z.-K., Shlyapnikov, G.V.: *Phys. Rev. A* **85**, 023614 (2012)
- Matveeva, N., Giorgini, S.: *Phys. Rev. Lett.* **109**, 200401 (2012)
- Seydi, I., Abedinpour, S.H., Tanatar, B.: *J. Low Temp. Phys.* **187**, 705 (2017)
- Seydi, I., Abedinpour, S.H., Asgari, R., Tanatar, B.: *Phys. Rev. A* **98**, 063623 (2018)
- Zinner, N.T., Bruun, G.M.: *Eur. Phys. J. D* **65**, 133 (2011)
- Sieberer, L.M., Baranov, M.A.: *Phys. Rev. B* **84**, 063633 (2011)
- Sun, K., Wu, C., Das Sarma, S.: *Phys. Rev. B* **82**, 075105 (2010)
- Yamaguchi, Y., Sogo, T., Ito, T., Miyakawa, T.: *Phys. Rev. A* **82**, 013643 (2010)
- Parish, M.M., Marchetti, F.M.: *Phys. Rev. Lett.* **108**, 145304 (2012)
- Abedinpour, S.H., Asgari, R., Tanatar, B., Polini, M.: *Ann. Phys. (N.Y.)* **340**, 25 (2014)
- Pines, D., Nozières, P.: *The Theory of Quantum Liquids*. W. A. Benjamin, Inc., New York (1966)
- Giuliani, G.F., Vignale, G.: *Quantum Theory of the Electron Liquid*. Cambridge University Press, Cambridge (2005)
- Jalabert, R., Das Sarma, S.: *Phys. Rev. B* **40**, 9723 (1989)
- Allmen, P.V.: *Phys. Rev. B* **20**, 345 (1992)
- Hwang, E.H., Das Sarma, S.: *Phys. Rev. B* **77**, 081412(R) (2008)
- Qaiumzadeh, A., Asgari, R.: *J. Phys.* **11**, 095023 (2009)
- Polini, M., Asgari, R., Borghi, G., Barlas, Y., Pereg-Barnea, T., MacDonald, A.H.: *Phys. Rev. B* **77**, 081411 (2008)
- Das Sarma, S., Hwang, E.H.: *Phys. Rev. B* **87**, 045425 (2013)
- Lischner, J., Vigil-Fowler, D., Louie, S.G.: *Phys. Rev. B* **89**, 125430 (2014)
- Lischner, J., Pálsson, G.K., Vigil-Fowler, D., Nemsak, S., Avila, J., Asensio, M.C., Fadley, C.S., Louie, S.G.: *Phys. Rev. B* **91**, 205113 (2015)
- Bostwick, A., Speck, F., Seylle, T., Horn, K., Polini, M., Asgari, R., MacDonald, A.H., Rotenberg, E.: *Science* **328**, 999 (2010)
- Principi, A., Asgari, R., Polini, M.: *Solid State Commun.* **151**, 1627 (2011)
- Godfrin, H., Mescheko, M., Lauter, H.J., Sultan, A., Böhm, H.M., Krotscheck, E.: *Nature* **483**, 576 (2012)
- Asgari, R., Davoudi, B., Polini, M., Guilian, G.F., Tosi, M.P., Vignale, G.: *Phys. Rev. B* **71**, 0453232 (2005)
- Asgari, R., Tanatar, B.: *Phys. Rev. B* **74**, 075301 (2006)
- Mahan, G.D. *Many-Particle Physics*, 3rd edn. Plenum Press, New York (2000)
- Krotscheck, E., Springer, J.: *J. Low Temp. Phys.* **132**, 281 (2003)
- Boronat, J., Casulleras, J., Grau, V., Krotscheck, E.: *J. Springer, Phys. Rev. Lett* **91**, 085302 (2008)

Publisher's Note Springer Nature remains neutral with regard to jurisdictional claims in published maps and institutional affiliations.